Journal of the European Ceramic Society **19** (1999) 2901–2908

PII: S0955-2219(99)00066-7
0955-2219/99/$ - see front matter

Shrinkage-free $ZrSiO_4$-ceramics: Characterisation and Applications

V. D. Hennige,[a]* J. Haußelt,[ab] H.-J. Ritzhaupt-Kleissl[b] and T. Windmann[b]

[a]Institut für Mikrosystemtechnik (IMTEK), Albert-Ludwigs-Universität, 79085 Freiburg, Germany
[b]Forschungszentrum Karlsruhe, Institut für Materialforschung III, 76344 Leopoldshafen, Germany

(Received 11 December 1998; accepted 27 February 1999)

Abstract

Dense, shrinkage-free $ZrSiO_4$-ceramics can be produced by a reaction-bonding process using $ZrSi_2$, ZrO_2, and a polysiloxane as starting materials. Sinter shrinkage is compensated by the volume increase during oxidation of $ZrSi_2$. In addition, the use of a Si-containing so called low-loss-binder [polymethylsilsesquioxane (PMSS)] reduces shrinkage further. Near net-shape ceramic compacts can be produced by an embossing process. As the green bodies are extremely dense but not brittle, they can be mechanically machined. The reaction-bonding process has to be controlled in a way that first the pyrolysis of PMSS, followed by the oxidation of $ZrSi_2$, and finally the formation of $ZrSiO_4$ and the sintering to dense compacts take place. Due to the absence of shrinkage and the good mechanical properties obtained, these ceramics open up new applications in fields requiring high dimensional accuracy such as microsystem engineering or dentistry. © 1999 Elsevier Science Ltd. All rights reserved

Keywords: $ZrSiO_4$, reaction bonding, precursors-organic, ZrO_2, near net-shape.

1 Introduction

The use of ceramic materials in technical applications is often limited because of the inevitable sinter shrinkage. In order to obtain the desired dimension of the parts, oversized moulds generally are used and often the sintered ceramic parts are machined by grinding. Particularly for applications where oversize of the mould or machining of the sintered part present severe technical or economical obstacles, e.g. special components in microsystem engineering or crowns and inlays in dentistry, new solutions must be developed. Due to the existing difficulties, the use of components made of structural ceramics is still exceptional in microsystem engineering.[1,2] Also in dentistry all-ceramic crowns still have a rather small market share because of their difficult production and their mechanical properties which are not yet optimal.[3–6] For these applications it is impossible to oversize the green compacts. There only exists an exact moulding die, e.g. a reproduction of a tooth stump. Due to this, green and sintered body must have exactly the same dimensions.

One possibility to solve the problem of sinter shrinkage is the so-called reaction-bonding process. During this process, one component undergoes a volume expansion reaction by which the sinter shrinkage is compensated. For example, shrinkage-free Al_2O_3-ceramics can be produced by using the reaction-bonded aluminium oxide process (RBAO) or other very similar techniques.[7–11] A minimization of sinter shrinkage is also known in the field of non-oxide ceramics. An example is the active filler controlled pyrolysis process (AFCP).[12,13]

The process described in this paper[14–16] uses an intermetallic compound [zirconium silicide ($ZrSi_2$)] as reactive component. Compared to the RBAO-process, where aluminium is used as reactive component, the intermetallic compound has two advantages. On the one hand, oxidation is combined with a much higher relative volume increase so that a relatively small volume fraction of this compound is necessary. On the other hand, the intermetallic compound is much less sensitive to oxidation, so that oxidation during the powder processing can be mostly avoided. As powder processing is to be carried out by a pressing or embossing process, polymethylsilsesquioxane (PMSS), a so-called low-loss-binder based on silicon, is used as binder. Compared to usually applied binders, the advantage of this binder is that it is not totally burnt-out during the pyrolysis in air or oxygen

---

*To whom correspondence should be addressed.

because it partially ceramizes. Consequently, sinter-shrinkage is further reduced. An oxide ceramic powder [zirconium oxide (ZrO_2)] serves as inert filling component, which finally reacts with the oxidation products of silicide and polysiloxane to form $ZrSiO_4$.

To exactly counterbalance the sinter-shrinkage to be expected, the necessary amount of the reactive component ($ZrSi_2$) has to be calculated. According to eqn (1), the linear shrinkage S of the body during sintering can be calculated:

$$S = \sqrt[3]{\left(1 + \Sigma \tilde{V}_i \Delta \tilde{V}_i\right) \frac{\tilde{\rho}_{\text{green}}}{\tilde{\rho}_{\text{sinter}}}} - 1 \tag{1}$$

with

$\tilde{V}_i$: volume fraction of the component i
$\Delta \tilde{V}_i$: rel. volume change of the component i
$\tilde{\rho}$: rel. green and sinter density of the bodies

If in eqn (1) the sinter shrinkage is set at zero ($S = 0$), the quantity of silicide can be calculated in a given system composed of a reactive component (silicide), binder (PMSS) and an inert filler (ZrO_2), if the values on the right side of eqn (2) are known:

$$\tilde{V}_{\text{silicide}} = \frac{\tilde{\rho}_{\text{sinter}}/\tilde{\rho}_{\text{green}} - \tilde{V}_{\text{binder}} \cdot \Delta \tilde{V}_{\text{binder}} - 1}{\Delta \tilde{V}_{\text{silicide}}} \tag{2}$$

The relative volume change of $ZrSi_2$ depends on the phases which are formed after the reaction. For the reaction

$$ZrSi_2 + 3O_2 \rightarrow ZrSiO_4 + SiO_2(q) \tag{3}$$

a theoretical value of $\Delta \tilde{V} = 106\%$ is obtained. The relative volume change of PMSS can be calculated following Ref. 17 by using ceramic yield and density changes.

2 Experimental Procedure

To manufacture the ceramics, $ZrSi_2$ (Johnson-Matthey; 99·5%) is milled for 48 h in hexane (ball mill, ZrO_2 milling-bowl and -balls) and then together with the ZrO_2 (Tosoh; TZ3Y) milled for another 24 h in hexane. After removing the hexane, the powder is suspended in ethanol, and the PMSS (ABCR), which is dissolved in ethanol, is added. In some cases a fraction of the PMSS is replaced by a conventional binder (polyvinylbutyrale, PVB; Aldrich). By spray-drying this suspension is converted into granulates which consist typically of about 35 vol% $ZrSi_2$, 35 vol% ZrO_2, and 30 vol% PMSS. This granulate can be densified to grey–black compacts by axial or isostatic pressing or embossing. Table 1 shows the composition of the ceramics mentioned in this paper.

Embossing of the powder can be carried out by using a metallic embossing die, such as for example for a coin, or by an adequately structured polymer die, for example one made of polymethylmethacrylate (PMMA).[18] If a metallic die is used, the green body is removed from the mould mechanically, in case of a PMMA die the "principle of the lost mould" is applied. Hereby the die is not removed mechanically from the green body but is pyrolyzed during the reaction sintering. Moreover, the green bodies that show an extremely high strength, can be further machined, for example by milling, drilling or grinding. In this way complex microparts can be produced from pre-shaped, cold isostatically pressed green bodies.

After the manufacturing of the green compacts, they are reaction-sintered in a high-temperature chamber furnace in flowing air. A characteristic temperature profile is shown in Fig. 3. In general, only the sintering time at maximal temperature of 1550–1600°C is extended up to 24 h. During the process, first PMSS is pyrolyzed, then $ZrSi_2$ is oxidized, and finally the ceramic is sintered to dense bodies. In order to compensate the sinter shrinkage ($S=0$), and taking into account the actually obtained sinter density, the density of the green body must be corrected by variation of the compacting pressure.

Processes occurring during the reaction sintering process are monitored by thermogravimetry (Netzsch STA 409) and dilatometry (Linseis L 75). The phase composition is analysed by X-ray powder diffractometry (XRD; Siemens D5000), the chemical composition is determined by X-ray fluorescent analysis (XFA; Siemens SRS 303). Porosity P is measured by a mercury porosimeter (CE-Instruments Porosimeter 4000). The maximal pressure of the porosimeter was 400 MPa, so only pores with a pore radius of larger than 2 nm could be detected. Mechanical properties are examined by a hardness tester (Vicker's hardness H; Leco V 100) and the four-point bending test (UTS 10T). With this bending test bending strength σ_B, fracture

Table 1. Ceramics mentioned in the text (starting composition)

	Volume fraction (vol%)			
Samples	*$ZrSi_2$*	*ZrO_2*	*PMSS*	*PVB*
Z_37·0/30	37·0	33·0	30	—
Z_34·8/30	34·8	35·2	30	—
Z_37·0/20 + 10	37·0	33·0	20	10
Z_38·8/20 + 10	38·8	31·2	20	10
Z_40·8/20 + 10	40·8	29·2	20	10

toughness k_{Ic} (notched samples) and Young's modulus Y are determined. Microstructural examination of the ceramics is carried out by scanning electron microscopy (SEM; JEOL JSM 6400).

3 Results and Discussion

3.1 Fabrication of the green body

As given by eqn (2), a certain variation of the starting volume fractions of $ZrSi_2$, ZrO_2, and PMSS—and thus of the obtainable final composition—of the shrinkage-free ceramics is possible. The relative volume changes of the educts are known. As already mentioned, the volume change of $ZrSi_2$ is 106%; for PMSS a ceramic yield of $\alpha_{\text{ker.}} = 81\%$ is obtained, and so a $\Delta\tilde{V}$ of −58% results.

Consequently, the fraction of $ZrSi_2$ necessary to compensate the shrinkage depends on the fraction of PMSS and on the relative green and sinter density. In the case of this work the sinter density to be reached is fixed at 95% of the theoretical density (TD). Thus the volume fraction of $ZrSi_2$ to compensate sinter shrinkage can be calculated from eqn (2). The result is shown in Fig. 1. The difference between 100 vol% and the amount of $ZrSi_2$ and PMSS is given by the inert component ZrO_2.

Figure 1 illustrates that theoretically there are many possible compositions to produce shrinkage-free ceramics. Practically, however, for a given volume fraction of binder only a limited range of the green density is attainable. With regard to the processing of the starting materials as well as to the obtained sinter densities the best results can be achieved when approximately the same volume fractions of the three components, $ZrSi_2$, ZrO_2 and PMSS are used. For these ceramics, the necessary green density ranges from 75 to 85% TD.

Equations (1) and (2) as well as Fig. 1 show that for a given composition of the green bodies and a constant sinter density, the necessary green density can be exactly evaluated. This green density must be reached by the pre-compaction process. In practice, typically green densities of approximately 65 to 85% TD—depending on the different compaction pressure—are obtained for the ceramics. As PMSS shows thermoplastic behaviour, the needed compaction pressure for a given green density can be significantly reduced by increasing the temperature during compaction. This is shown in Fig. 2 with Z_38·8/20 + 10 as an example.

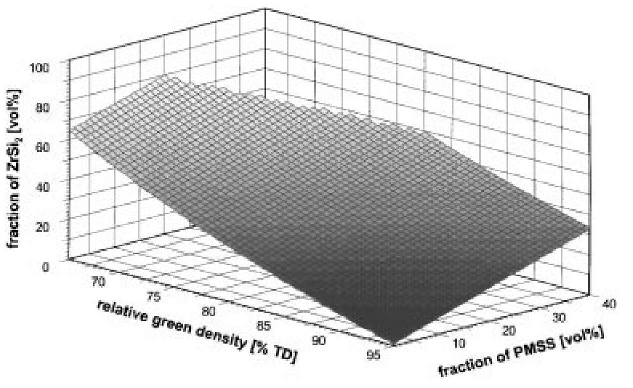

Fig. 1. Volume fraction of PMSS necessary to compensate sinter shrinkage in the system $ZrSi_2$–ZrO_2–PMSS (with $\tilde{\rho}_{\text{sinter}} = 95\%$ TD).

As can be seen from Fig. 2, in the case of Z_38·8/20 + 10 at room temperature the necessary green density for $S = 0$, i.e. 79·5% TD, cannot be achieved at reasonable pressures (< 350 MPa). Due to the thermoplastic behaviour of the PMSS, the green density increases significantly when the temperature is raised at a given pressure, e.g. from 74·5% TD at 25°C to 82·5% TD at 120°C and a constant pressure of 270 MPa. So the necessary green density can be achieved in all cases by pressing at elevated temperatures (80–100°C) and pressures below 350 MPa.

The compressibility of the granulate is not only influenced by the compaction temperature but also depends to a great extent on the types and amounts of binder used. Depending on the characteristics of the PMSS, that is whether it has small or large amounts of low-molecular fractions, the compressibility is poorer or better. Poorer compressibility, as encountered with the mentioned Z_38·8/20 + 10 ceramics, requires the use of a further binder (PVB) and densification at higher temperature of up to 120°C.

3.2 Analysis of the reaction-bonding process

Thermal analysis is the most important method to examine the reaction-bonding process. The simultaneous thermal analysis monitors the pyrolysis of PMSS which is accompanied by a mass decrease and the oxidation of $ZrSi_2$ that leads to a mass increase. The sintering process (length decrease) and the oxidation of $ZrSi_2$ (length increase) can be observed by dilatometry. Figure 3 shows the behaviour of a green body during a typical thermal treatment, taking Z_37·0/30 as example.

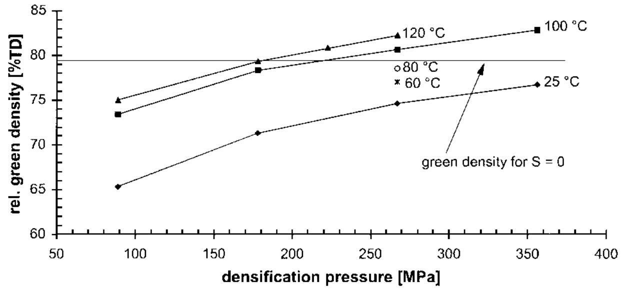

Fig. 2. Compressibility of the granulate Z_38·8/20 + 10 as a function of temperature.

Up to a temperature of about 600°C, pyrolysis of PMSS into SiO_2 takes place. In this temperature range length and mass show only minor changes. From the thermal hold at 650°C onwards, oxidation of $ZrSi_2$ into ZrO_2 and SiO_2 is continuously progressing, as can be seen by the mass and length increase. The formation of $ZrSiO_4$ begins already at a temperature of about 1100°C and the sintering process starts. Now the body begins to shrink, however, the mass is still increasing. At a temperature of 1300°C, oxidation is completed. The X-ray diffraction analysis reveals that there is no $ZrSi_2$ left and the mass of the body does not change anymore. Most of ZrO_2 and SiO_2 have transformed into $ZrSiO_4$. After a further temperature increase of up to 1600°C, this transformation is almost complete. At the end, white bodies with a density of about 92% TD whose linear shrinkage is approximately zero are found. The value of the here mentioned theoretical density is based on thermodynamic calculations and is related to a theoretical composition of the ceramic of x% $ZrSiO_4$ and (100−x)% ZrO_2 or SiO_2. A detailed explanation is given in the following chapter. In the given sample shown in Fig. 3, there is a final expansion of just below 1% after sintering, as sintering was limited to 4 h. If sintering time is prolonged to 12 or even 24 h, the shrinkage can be reduced to $S=0$.

The described phase composition of the bodies in the respective regions of the reaction bonding process can be revealed by XRD analysis. Figure 4 gives an overview.

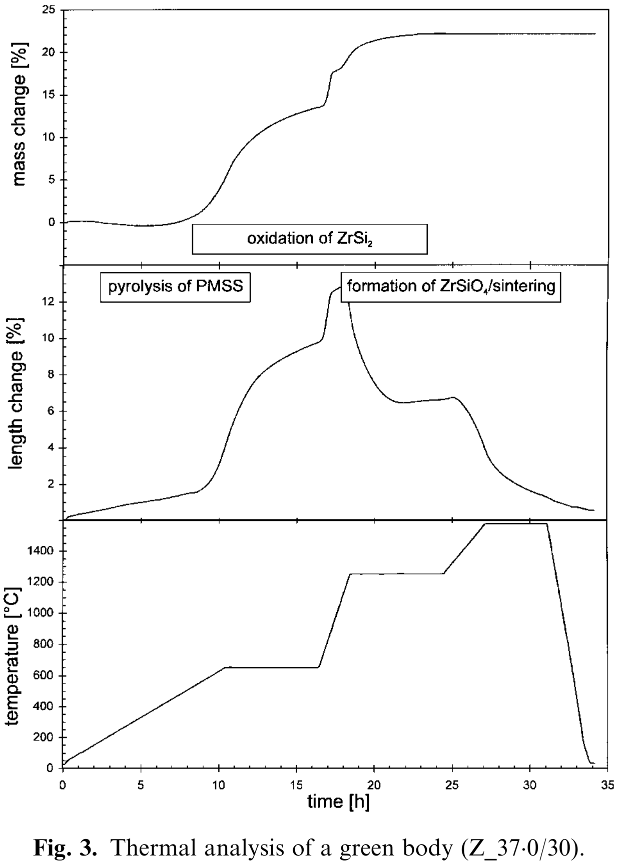

Fig. 3. Thermal analysis of a green body (Z_37·0/30).

Regarding the results given by thermal analysis and XRD analysis the processes occurring during the thermal treatment of the bodies can be summarised as follows:

$$T < 600^\circ\mathrm{C}: \quad [\mathrm{Si(CH_3)O_{1,5}}]_n \xrightarrow{\mathrm{air}} \mathrm{SiO_2} + \ldots \tag{4}$$

$$T \geq 500^\circ\mathrm{C}: \quad \mathrm{ZrSi_2} \xrightarrow{\mathrm{air}} \mathrm{ZrO_2} + 2\ \mathrm{SiO_2} \tag{5}$$

$$T > 1100^\circ\mathrm{C}: \quad \mathrm{ZrO_2} + \mathrm{SiO_2} \rightarrow \mathrm{ZrSiO_4} \tag{6}$$

In the detailed representation of the process (Fig. 3) the three reaction regimes pyrolysis of PMSS [eqn (4)], oxidation of $ZrSi_2$ [eqn (5)], formation of $ZrSiO_4$ [eqn (6)] and sintering process are indicated.

Furthermore, the open porosity of the bodies changes considerably during the reaction-bonding process, as can be seen from Fig. 5. The green bodies have only a very low porosity because of the high green density of more than 80% TD. Porosity increases with increasing temperatures because of the pyrolysis of PMSS. At 900°C porosity reaches its maximum of about 36%, a result which is in accordance with theoretical values. This confirms

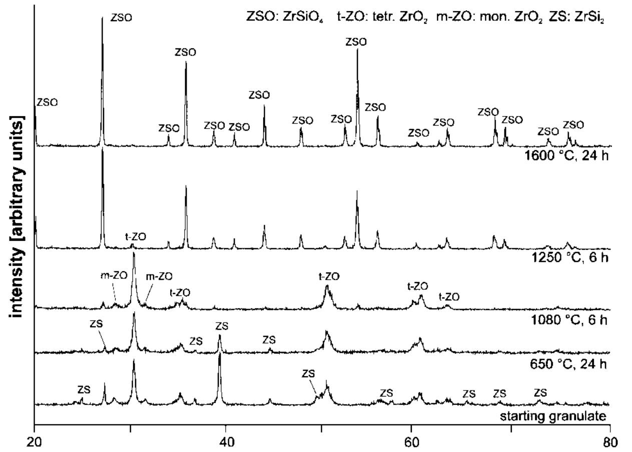

Fig. 4. XRD analysis of compacts (Z_37·0/30) after different thermal treatment.

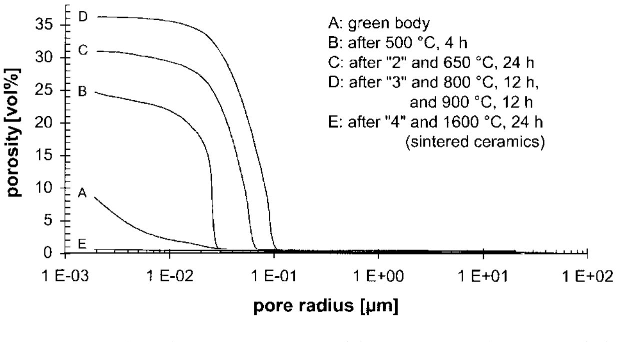

Fig. 5. Porosity changes (measured by Hg-porosimetry) of the compacts during the thermal treatment (Z_38·8/20 + 10).

the results that up to this temperature, sintering can be ignored. The sintered samples (1600°C, 24 h) show only a very small open porosity of about 0·5 to 1 vol%.

Open porosity is extremely important during the reaction bonding process. In the presence of open porosity, oxygen transport can occur by gas diffusion mechanisms instead of bulk diffusion mechanisms. If the sintering process starts too early, when oxidation is not yet completed, oxidation inside the bodies is considerably slowed. A further increase of temperature leads to a new acceleration of oxygen transport and to further oxidation. As this is coupled with a volume increase, the already densified oxide surface layer of the compacts tends to crack and the body is destroyed. Therefore, a temperature profile exactly fitted to the reaction-bonding process is indispensable for the fabrication of highly dense and crack-free ceramics. This profile can be obtained by thermal analysis.

3.3 Characterisation of the ceramics

At the end of the reaction-bonding process all investigated ceramics should mainly consist of $ZrSiO_4$. Small amounts either of SiO_2 or ZrO_2 are to be expected as secondary components. According to thermodynamics, $ZrSiO_4$ is the stable modification,[19] therefore after the thermal treatment ZrO_2 and SiO_2 should not coexist at room temperature.

Stoichiometry, that is the ratio of ZrO_2/SiO_2, is monitored by X-ray fluorescent analysis. It shows that the ceramics possess in fact the ratio of ZrO_2/SiO_2 expected on the basis of the starting composition. The results obtained are shown in Table 2.

In all samples the fraction of ZrO_2 is slightly higher than expected. This can be explained by ZrO_2-impurities introduced into the powder during the milling process (wear of the ZrO_2-milling-bowl and -balls).

As can already be seen from Fig. 4, $ZrSiO_4$ is the main component of the ceramics as detected by XRD analysis. However, examinations of all ceramics show that the phase composition does not exactly correspond to the predictions of Table 2. Figure 6 shows the comparison of three typical ceramics.

Table 2. Chemical analysis (XFA) of the ceramics

Ceramic	*ZrO_2-fraction*[a]	*SiO_2-fraction*[a]	*Expected phases*
Z_37·0/20 + 10	51·2 (50·0)[b]	48·8 (50·0)	$ZrSiO_4$ (+ZrO_2)
Z_38·8/20 + 10	49·8 (48·7)	50·2 (51·3)	$ZrSiO_4$ (+SiO_2)
Z_40·8/20 + 10	48·9 (47·4)	51·1 (52·6)	$ZrSiO_4$ (+SiO_2)

[a] In (mol%).
[b] Values in brackets: expected due to starting composition.

Due to stoichiometry and thermodynamic considerations all ceramics in Fig. 6 should show no free ZrO_2. For example, in case of Z_38·8/20 + 10 there is a higher amount of SiO_2 than ZrO_2 detected by XFA (see Table 2). So one should expect that after the formation of $ZrSiO_4$ a small amount of free SiO_2 rests. In contrast to that, by XRD analysis $ZrSiO_4$ and ZrO_2 can be observed; SiO_2 cannot be detected because it is amorphous. This means that the transformation of SiO_2 and ZrO_2 has not occurred completely. This observation is confirmed by the microscopic examination of the microstructure (Fig. 7) which can be amplified by EDX-analysis.

As expected, the medium grey matrix is composed of $ZrSiO_4$. The white phase is ZrO_2 and the black phase SiO_2. In addition, the sample contains some small pores. A quantitative phase analysis with an image-analysing system reveals a fraction of about 84 vol% $ZrSiO_4$, 9·5 vol% SiO_2, 5 vol% ZrO_2 as well as 1·5 vol% porosity. So far, the reasons for the simultaneous occurrence of all three phases have not been totally clarified. Even with very long sintering times of up to 24 h, a complete transformation of ZrO_2 and SiO_2 into $ZrSiO_4$ could not be achieved. This is in accordance with

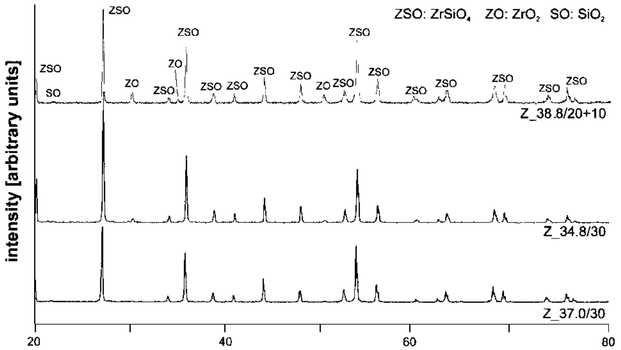

Fig. 6. Comparison of XRD analysis of selected ceramics (after sintering).

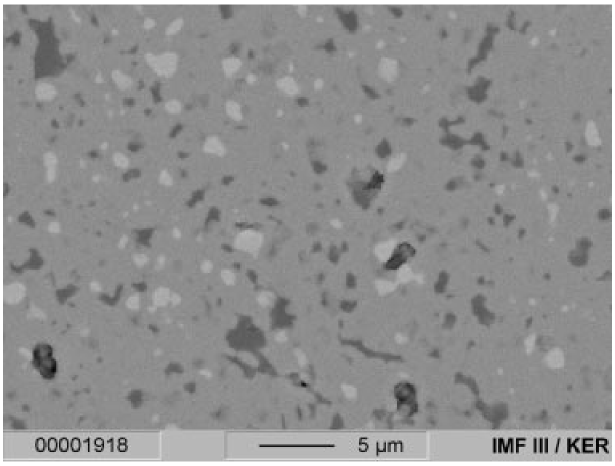

Fig. 7. SEM-image of a Z_38·8/20 + 10 ceramic (material contrast, phase composition, see text).

the results of other authors.[20] Instead of long sintering times it is very difficult to achieve a complete conversion of ZrO_2 and SiO_2 to $ZrSiO_4$. Because sintering temperature of 1550°C is about 180°C below the peritectic decomposition temperature[19] and local excursions in temperature as a consequence of reaction heats (e.g. oxidation of $ZrSi_2$) are not to be expected in this temperature region, $ZrSiO_4$ should be stable at these conditions.

The physical and mechanical properties of the ceramics are important for their use in microsystem engineering or dental applications. Table 3 lists the most important properties.

The density of the ceramics ranges from 91 to 93% TD. However, it must be noted that the theoretical density has been calculated assuming a total transformation of ZrO_2 and SiO_2 into $ZrSiO_4$. As this is not the case, the actual relative density is slightly higher than indicated in Table 3. This explains why porosity of less than 1 vol% was found by Hg-porosimetry.

The bend strength σ_0, the Weibull modulus m and the fracture toughness k_{Ic}, were determined using samples with additional PVB as binder. The results indicate that the mechanical properties depend on the composition. An increasing ZrO_2 fraction of the ceramic slightly increases the strength σ_0 and the Young's modulus. The average bend strength of the ceramic ranges from 190 to 220 MPa. The Weibull modulus m varies between 10 and 20. The fracture toughness depends only slightly on the composition and is just below $2{\cdot}5\,\mathrm{MPa}\sqrt{m}$. Comparative studies on fracture toughness using the less reliable indentation method confirmed these values.

Besides attaining satisfactory mechanical properties of the ceramics, shrinkage-free microparts were successfully manufactured. Figure 8 shows a comparison between a ceramic produced with a metallic stamping die and the die itself. Figure 9 shows a shrinkage-free micropart which was manufactured with a polymeric embossing die. In both cases the dimensions of the sintered parts were identical to those of the embossing dies. Finally, Fig. 10 shows some microparts manufactured out of isostatically pressed green compacts by mechanical machining.

Fig. 8. Comparison of the stamping die (in the middle) green body (right) and sintered ceramic (left).

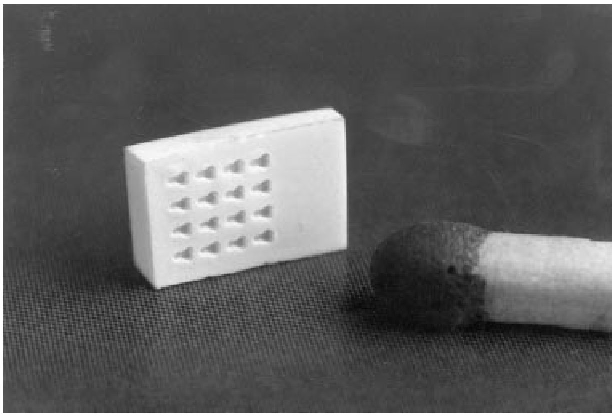

Fig. 9. $ZrSiO_4$ micropart manufactured by using a PMMA die.

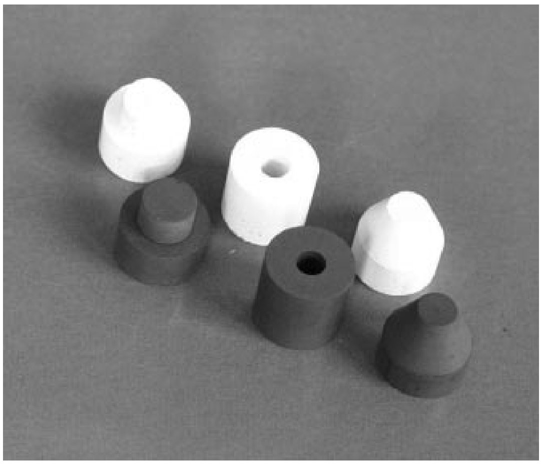

Fig. 10. Microparts manufactured by mechanical machining methods (above: sintered compacts; below: green compacts).

Table 3. Survey of the physical and mechanical properties of the ceramics

Sample	ρ_{sinter} *(g/cm³)*	$\rho_{sinter}{}^{c}$ *(% TD)*	P *(vol%)*	$\sigma_{4P}{}^{a}$ *(MPa)*	*Y* *(GPa)*	$\sigma_0{}^{b}$ *(MPa)*	m^{b}	k_{Ic} *(MPa√m)*	H *(HV 5)*
Z_37·0/30	4·21	90·9	—	209	181	—	—	—	800
Z_34·8/30	4·35	92·6	< 1	215	192	—	—	—	850
Z_37·0/20 + 10	4·32	91·9	< 1	207	196	216	10·8	2·49	880
Z_38·8/20 + 10	4·23	91·2	< 1	189	185	196	15·3	—	810
Z_40·8/20 + 10	4·17	91·2	< 1	185	177	189	19·9	2·38	785

[a] Average.
[b] According to Weibull statistic.
[c] Related to the initially calculated phase composition.

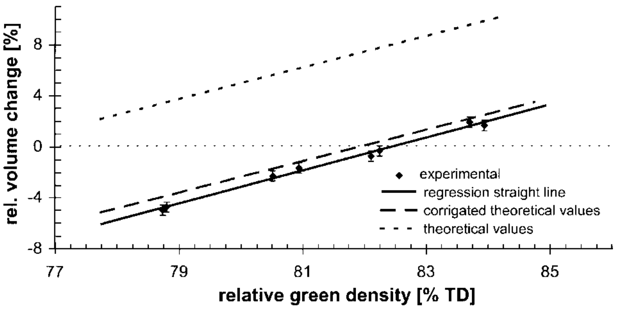

Fig. 11. Relative volume change of Z_38·8/20 + 10-ceramics as a function of the green density (see text).

3.4 Examination of the sinter shrinkage

Finally, the most important aspect of this paper, the examination of the sinter shrinkage will be treated more closely. The results of the thermal analysis in Fig. 3 already illustrate that shrinkage-free and dense ceramics with good mechanical properties can be manufactured by the process described in this paper. The example of Z_38·8/20 + 10 in Fig. 11 reveals how the relative volume change of the green compact depends on the green density. Hereby the obtained sinter density is independent of the composition and lies at about 91% TD. This illustration contains two additional straight lines. The dotted line marks the theoretical dependence of the relative volume change on the green density. The experimental values for the volume fraction of the components and their theoretical relative volume changes were used as parameters, the sinter density was fixed at 91·5% TD. The dashed line is a correction of the model. A smaller volume increase of $ZrSi_2$ is taken into account due to ZrO_2 impurities and the oxidation which partially occurs during powder processing. In addition, the theoretical density corrected on the basis of the structure evaluation is applied (see Fig. 7 and text above). Consequently, the relative volume change of the $ZrSi_2$ is not 106% but only 98·4%. On the basis of the already mentioned analysis, the theoretical density of the Z_38·8/20 + 10 ceramic diminishes from 4·64 to 4·51 gcm^{-3}, the relative sinter density increases accordingly to 94% TD.

Figure 11 illustrates that by correcting the data used in eqn (1) the experimental and the theoretical data correspond within the margin of error of the determined experimental data.

4 Summary and Conclusion

Dense and shrinkage-free $ZrSiO_4$ ceramics were produced by a reaction-bonding process based on ZrO_2, $ZrSi_2$ and PMSS as starting materials. The sinter shrinkage was compensated by a volume increase during the oxidation of $ZrSi_2$ forming ZrO_2 and SiO_2. As PMSS, a so-called low-loss binder, was used as compacting help, only a relatively small fraction of $ZrSi_2$ had to be used. Furthermore, by a combined pressing/embossing process near net-shape ceramic compacts were successfully produced. The as-manufactured green bodies can be easily machined. As the sintered $ZrSiO_4$-ceramics display satisfactory mechanical properties they open up new fields of application.

Owing to the advantages described in this paper, this process is suited for the production of microparts and components for microsystem engineering. According to specific needs, microparts with identical dimensions before and after sintering can be produced. Machining of the sintered ceramics, which is impossible in micrometer dimensions, is not necessary.

Dentistry is another potential field of application. By the described reaction-bonding process all-ceramic crowns and inlays can be manufactured. The white colour and the good mechanical properties of the ceramics, which are comparable to those of materials already in use,[3] are further advantages. Because of the white colour, porcelain or composite veneering, indispensable for aesthetic reasons, should be possible without problems.

References

1. Bauer, W., Knitter, R., Ritzhaupt-Kleissl, H.-J. and Haußelt, J., Ceramic microcomponents and their applications in microsystems engineering. *MST News*, 1997, **19**, 26–27.
2. Bauer, W., Ritzhaupt-Kleissl, H.-J. and Haußelt, J., Micropatterning of ceramics by slip pressing. *Ceramics International*, 1999, **25**, 201–205.
3. Bieniek, K. W. and Marx, R., Die mechanische Belastbarkeit neuer vollkeramischer Kronen- und Brückenmaterialien. *Schweizer Monatsschrift für Zahnmedizin*, 1994, **104**, 284–289.
4. Hopp, M., Klinisch-biologische Betrachtung zum In-Ceram-System. *Dentallabor*, 1994, **XLII**, 665–670.
5. Geis-Gerstorfer, J. and Kanjantra, P., Zum Einfluß der Prüfmethode auf die Biegefestigkeit von IPS-Empress und In-Ceram. *Deutsche Zahnärztliche Zeitung*, 1992, **47**, 618–621.
6. Luthardt, R., Herold, V., Sandkuhl, O., Reitz, B., Knaak, J. P. and Lenz, E., Kronen aus Hochleistungskeramik. *Deutsche Zahnärztliche Zeitung*, 1998, **53**, 280–285.
7. Wu, S., Holz, D. and Claussen, N., Mechanisms and kinetics of reaction-bonded aluminium oxide ceramics. *Journal of the American Ceramic Society*, 1993, **76**, 970–980.
8. Holz, D., Pagel, S., Bowen, C., Wu, S. and Claussen, N., Fabrication of low-to-zero shrinkage reaction-bonded mullite composites. *Journal of the European Ceramic Society*, 1996, **16**, 255–260.
9. Takeshita, M., Kurita, S. and Iwaishi, H., Methode zur Herstellung von keramischen Zahnkronen. *Japanische Offenlegungsschrift* 1991, *Hei 3-198 842* (translation).
10. Zhang, C., Vlajic, M. D., Krstic, V. D. and Hasselmann, D. P. H., Sintering and thermal conductivity of low shrinkage Al_2O_3 based ceramics. *Science of Sintering*, 1996, **28**, 165–173.
11. Suttor, D., Klebe, H.-J. and Ziegler, G., Formation of mullite from filled siloxanes. *Journal of the American Ceramic Society*, 1997, **10**, 2541–2548.

12. Erny, T., Seibold, M., Jarchow, O. and Greil, P., Microstructure development of oxycarbide composites during active-filler-controlled polymer pyrolysis. *Journal of the American Ceramic Society*, 1993, **76**, 207–213.
13. Seibold, M. and Greil, P., Thermodynamic and microstructural development of ceramic composite formation by active filler-controlled pyrolysis (AFCOP). *Journal of the European Ceramic Society*, 1993, **11**, 105–113.
14. Hennige V. D., Ritzhaupt-Kleissl H.-J. and Hauβelt, J., Verfahren zur Herstellung eines oxidkeramischen Sinterkörpers und dessen Verwendung. Deutsches Patent DE 195 47 129, 1995.
15. Hennige, V. D., Ritzhaupt-Kleissl, H.-J. and Hauβelt, J., Herstellung von $ZrSiO_4$-Keramiken mit minimiertem Sinterschrumpf. *Keramische Zeitschrift*, 1998, **50**, 262–265.
16. Hennige, V. D., Verfahrens- und Werkstoffentwicklung zur Herstellung oxidkeramischer Mikroformteile mit minimiertem Sinterschrumpf. Shaker Verlag, Herzogenrath, 1998.
17. Greil, P. and Seibold, M., Modelling of dimensional changes during polymer-ceramic conversion for bulk component fabrication. *Journal of Materials Science*, 1992, **27**, 1053–1060.
18. Ruprecht, R., Bacher, W. and Piotter, V., Abformen mit ungefüllten und gefüllten Kunststoffen. In *Proceedings of the 2nd Statuskolloquium des Projekts Mikrosystemtechnik*, Forschungszentrum Karlsruhe. *FZKA* 1995, **5670**, 145–150.
19. Buttermann, W. C. and Foster, W. R., Zircon stability and the ZrO_2–SiO_2 phase diagram. *The American Mineralogist*, 1967, **52**, 880–885.
20. Spearing, D. R. and Huang, J. Y., Zircon synthesis of milled SiO_2 and ZrO_2. *Journal of the American Ceramic Society*, 1998, **81**, 1964–1966.